WATER RESOURCES RESEARCH, VOL. 33, NO. 4, PAGES 639–648, APRIL 1997

Bacteriophage and microsphere transport in saturated porous media: Forced-gradient experiment at Borden, Ontario

Roger C. Bales, Shimin Li,[1] and T.-C. Jim Yeh
Department of Hydrology and Water Resources, University of Arizona, Tucson

Melissa E. Lenczewski[2] and Charles P. Gerba
Department of Soil, Water and Environmental Science, University of Arizona, Tucson

Abstract. A two-well forced-gradient experiment involving virus and microsphere transport was carried out in a sandy aquifer in Borden, Ontario, Canada. Virus traveled at least a few meters in the experiment, but virus concentrations at observation points 1 and 2.54 m away from the injection well were a small fraction of those injected. A simplified planar radial advection-dispersion equation with constant dispersivity, coupled with equilibrium and reversible first-order mass transfer, was found to be adequate to simulate the attachment and transport process. During the experiment a short-duration injection of high-*p*H water was also made, which caused detachment of previously attached viruses. For simulating this detachment and associated transport, the same transport and mass-transfer equations were used; but all rate parameters were varied as groundwater *p*H changed from 7.4 to 8.4 and then back to 7.4. The physicochemical parameters obtained from fitting breakthrough curves at one sampling well were used to predict those at another well downstream. However, laboratory-determined parameters overpredicted colloid removal. The predicted pattern and timing of biocolloid breakthrough was in agreement with observations, though the data showed a more-disperse breakthrough than expected from modeling. Though clearly not an equilibrium process, retardation involving a dynamic steady state between attachment and detachment was nevertheless a major determinant of transport versus retention of virus in this field experiment.

Introduction

The occurrence and transport of human enteric viruses and bacteria in and through groundwater have been a long-standing public concern. Questions of virus transport are central to groundwater wellhead protection. Distances between virus sources such as septic tanks and drinking water wells are typically set on the basis of empirical relations. Quantitative estimates based on site-specific characteristics or transport modeling have not been used for setting groundwater protection standards.

Physical and mathematical models for describing the fate of biocolloids (i.e., virus and bacteria) in porous media have been suggested for more than a decade [e.g., *Vilker*, 1978; *Vilker and Burge*, 1980; *Funderburg et al*., 1981; *Grosser*, 1985; *Corapcioglu and Haridas*, 1984, 1985; *Yates et al*., 1987; *Matthess et al*., 1988; *Harvey and Garabedian*, 1991]. However, application of these models has suffered in part from a lack of systematic field and laboratory research. Accumulation of experimental data and validation of existing or newly developed models with data are essential.

The major factors controlling virus and bacteria fate in subsurface porous media are attachment to and detachment from the porous medium surfaces, growth and inactivation, and advection and dispersion [*Bales et al*., 1991; *Gerba et al*., 1991; *Harvey*, 1991]. Advection depends on groundwater velocity. Dispersion depends on velocity and aquifer heterogeneity and is scale dependent. Attachment and detachment rates are sensitive to groundwater chemical conditions, such as *p*H, ionic strength, and the composition of the porous media [*Gerba*, 1984; *Bales et al*., 1993], and in many cases are the most important factors controlling bacteria and virus transport. Inactivation of viruses depends strongly on temperature [*Yates et al*., 1987] and is typically slow compared to the rates of advection, attachment, and detachment [*Bales et al*., 1995]. Accurate prediction of virus transport through porous media near their source therefore often depends solely on the correct evaluation of the rates at which viruses attach to or detach from the porous medium surfaces.

This research was aimed at evaluating mathematical descriptions of the chemical and microphysical factors controlling biocolloid transport through porous media. We undertook a forced-gradient field experiment and subsequent mathematical modeling with three main questions in mind: (1) Can we model virus (bacteriophage) and microsphere transport at the field scale using the same few microscale parameters as have been used in the laboratory?, (2) How do colloid attachment to and detachment from aquifer media affect transport relative to that of a conservative solute in a heterogeneous system?, and (3) How does a disturbance in groundwater *p*H facilitate further transport of previously retained bacteriophage or microspheres. We used bacteriophage and microspheres rather than animal virus or bacteria because our primary aim was model testing. With these model colloids we have better experimental

[1]Now at Arizona Department of Environmental Quality, Phoenix.
[2]Now at Amway Corporation, Ada, Michigan.

Paper number 97WR00025.
0043-1397/97/97WR-00025$09.00

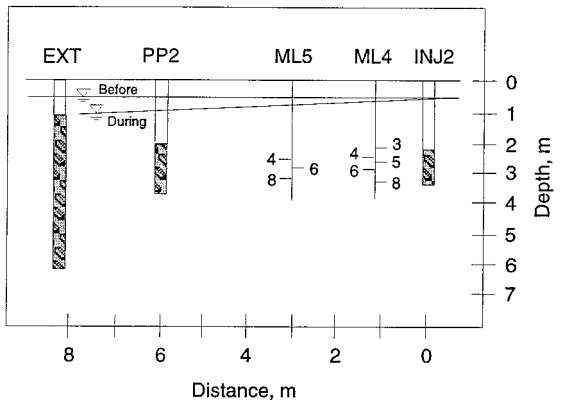

Figure 1. Portion of well system for field test at Borden, Ontario: cross-section view. Screened sections of extraction (EXT), partially penetrating (PP2), and injection (INJ2) wells for this experiment are shaded. To the left of EXT was a second injection (INJ1) well and a partially penetrating well that were used in the concurrent pesticide-transport experiment (not shown). ML4 and ML5 were multilevel monitoring wells; only the depths sampled are shown. Water table levels during and before experiment are also shown.

control and detection. We also used multiple colloids in order to compare their relative behavior.

Site Description

The test site was within an inactive sand quarry at the Canadian Forces Base, Borden, Ontario. The aquifer at the site is unconfined and composed of clean, well-sorted, fine- to medium-grained sand with distinct horizontal bedding evident [*Mackay et al*., 1986; *Sudicky*, 1986]. The thickness of the aquifer is about 9 m, and the ground surface is almost horizontal. On the bottom of the aquifer is a thick, silty clay deposit. The dry bulk soil density is 1.81 g cm^{-3}, with a solids density of 2.71 g cm^{-3} and specific surface area of 0.8 m^2 g^{-1} [*Mackay et al*., 1986]. Organic-carbon content (0.03%) and cation-exchange capacity (0.5 meq g^{-1}) are low, with a clay-size fraction near zero (reported as 0–15%). Dominant ions in the aquifer were Ca^{2+} and HCO_3^-, with *p*H of 7.4–7.5.

The measured hydraulic conductivities of 1279 samples from 32 cores measured with a falling head permeameter varied over more than 1 order of magnitude and indicated a horizontal layered structure; the overall geometric mean of the hydraulic conductivity (corrected to 10°C) is 7.2×10^{-5} m s^{-1} [*Sudicky*, 1986].

The natural hydraulic gradient at the site has been observed to range from 0.0035 to 0.0054 through the year [*MacFarlane et al*., 1983]; the best estimate of an average hydraulic gradient is 0.0043 [*Mackay et al*., 1986; *Sudicky*, 1986]. Averaged natural groundwater velocity was 0.09 m d^{-1} [*Mackay et al*., 1986]. The effective porosity was estimated to be approximately 0.3, that is, on the order of 90% of the estimated total porosity [*Mackay et al*., 1986]. Both slight and significant seasonal changes in the natural flow direction had been observed by different researchers [*MacFarlane et al*., 1983]. The water table was found to be very sensitive to rains, fluctuating between 0.5 and 1.0 m from ground surface in response to the rains during our field test.

The whole well system consists of one extraction well, one supply well, and two injection wells (Figure 1). Two field experiments were conducted at the same time: a virus-transport test involving injection well 2 and a pesticide transport test. *Mackay et al*. [1994] reported results of an earlier organic solute transport experiment at the site.

The extraction well was partially penetrating with a screened length of 5 m, slot size of 0.5 mm, and a total length of 6.2 m. The supply well was also partially penetrating, with a screened length of 1.5 m, slot size of 0.5 mm, and total length of 3.7 m. The injection well was partially penetrating with a screened length of 1.35 m and 0.25-mm slot size. The inner diameter of the extraction, supply, and injection wells was 51 mm.

There were 20 water table observation wells scattered around the test site, and 18 piezometers aligned with three straight lines in the radial direction of the extraction well within 30 m of the extraction well. These observation wells and piezometers were designed and installed by previous research groups. Each observation well was made of 25–38 mm diameter PVC pipes, fitted with a length of nylon screened open section made according to the estimated drawdown at each point. Piezometers were similar, but had a consistent 0.2-m length of nylon-screened open section. Piezometers were designed to measure drawdown at a "point," while water table observation wells were designed to measure an average drawdown over a finite vertical distance.

The water table was monitored with a tape each day during the experiment at both piezometers and observation wells after the extraction was started. More-frequent observations were made at a few piezometers close to the extraction well at the beginning of the extraction, since drawdown at early times was very fast. There were rain events during the experiment; measurements were made immediately after each rain to monitor the effect on the water table.

At the extraction well a centrifugal pump was installed to maintain a large hydraulic gradient at the site. A flowmeter was used to measure the instantaneous flow rate. The extracted water was discharged to a pond about 200 m away from the site to avoid any disturbance to the local flow field. Water withdrawn from the supply well was reinjected to the aquifer through the two injection wells. The flow rate at the extraction well was 30 L min^{-1}. The maximum flow rate at the supply well was 5 L min^{-1}. Flow rates were 2 L min^{-1} at INJ2 and 3 L min^{-1} at INJ1.

Methods

The study, carried out in July 1991, consisted of two sequential experiments; in the first, attachment of colloids to aquifer media dominated, and in the second, detachment as well as attachment was important. For the first (attachment) experiment the injection mixture contained phages PRD-1 and M-1, polystyrene microspheres, and NaCl as a conservative tracer. The phage and microsphere solutions were made with 5 mL of 0.1-μm microspheres (9.82×10^{13} microspheres mL^{-1}), 10 mL of PRD-1 (1.24×10^{12} plaque-forming units (pfu) mL^{-1}), 10 mL of M-1 (10^{10} pfu mL^{-1}) and 3 L of distilled water. For the second (detachment) experiment the injection solution was high-*p*H water with no phage or microspheres. Sodium phosphate (Na_2HPO_4) was used to prepare the high-*p*H buffer, and NaOH was used to adjust the *p*H first to 8.6 and later to 10.0 in the injectate, after we found a *p*H of 8.6 was not adequate to raise the *p*H at the injection well because of dilution.

PRD-1 was obtained from J. Hsieh (Department of Microbiology and Immunology, College of Medicine, University of Arizona, Tucson). Bacteriophage PRD-1 is an icosahedral (20

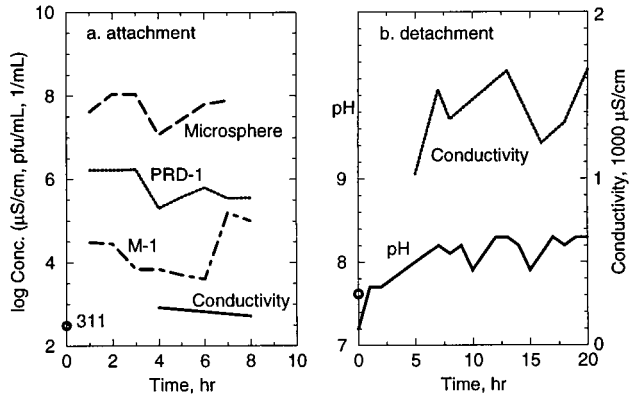

Figure 2. Injection history at injection well 2 (a) for attachment and transport experiment and (b) for detachment and transport experiment. Note background conductivity was 311 μS cm^{-1}. C_0 values taken as 1.1×10^8 mL^{-1} for microsphere, 1.7×10^6 pfu mL^{-1} for PRD-1, and 1.6×10^5 pfu mL^{-1} for M-1.

triangular faces) lipid phage with an average diameter of 62 nm [*Olsen et al*., 1974]. Its isoelectric point in calcium phosphate buffer (10^{-4} M Ca) is between *p*H 3 and 4 [*Bales et al*., 1991]. PRD-1 is a member of the Tectivirdae, a group of double-strained DNA somatic viruses composed of an outer protein coat that encloses a protein-lipid membrane vesicle [*Bamford et al*., 1981]. The lipid is not exposed on the surface of the phage. Two proteins make up the protein coat of the virus 43.1 and 34.3 kda in molecular mass. Both appear as homomultimers where the subunits are strongly bound together. The amino acid sequence of protein P5 appears in a collagenlike motif. Additional information on the structure of PRD-1 is given by *Bamford et al*. [1995].

M-1 is a heat-resistant bacteriophage that was isolated in our laboratory from Tucson sewage. The M-1 virus is a typical T-even double-stranded phage with a head, tail, base plate, and tail fibers belonging to the genus Mycoviridae. It is a somatic phage that attaches to the cell wall of the host bacteria by a base plate. The head of the phage is an icosahedron, elongated by one or two extra bands of hexamers of 85×110 nm. Its shell consists of 5-nm-diameter capsomers composed mainly of three proteins of molecular weights of 46 and 960 amino acids. The contractile tail (25×110 nm) is composed of a tube, sheath, and connecting tail with a collar and whiskers, with a complex base plate with tail fibers. A detailed description of the composition of the structural proteins is given by *Frankel-Conrat et al*. [1988]. Attachment to inanimate surfaces is usually by the head or tail. The pH_{iep} of the phage is 4–5 [*Gerba*, 1984].

Microspheres were 100-nm monodispersed uncharged polystyrene beads containing yellow-green fluorescent dye (coumarin excitation maximum, 458 nm; emission maximum, 540 nm), from Polysciences, Inc., Warrington, Pennsylvania.

The host bacteria were Salmonella typhimurium LT2 for PRD-1 and Escherichia coli (ATTC 15597) for M-1. The phages were assayed by the pfu methods as described by *Adams* [1959]. All virus assays were performed in duplicate. Replicate assays of a single sample for phage differed by an average of 25% for all samples. A detailed description of the phage assay is given by *Bales et al*. [1991]. The microspheres were enumerated on polycarbonate membrane filters (Nuclepore, Pleasanton, California) with a pore size of 0.05 μm and a diameter of 25 mm using epifluorescent microscopy. Filters were rendered black by soaking for 24 hours in a solution of 2 of Irgalan black dissolved in 1 L of 2% acetic acid, then rinsed with distilled water and dried [*Hobbie et al*., 1977]. Each sample was sonicated for 20 min to break up aggregates; then 1–10 mL of sample was vacuum filtered to deposit colloids. Filters were then placed on glass slides with a drop of glycerol and read using an Olympus BH-2 microscope (Olympus Optical Co., Tokyo, Japan) fitted with epifluorescence. We observed the emission from a 0.1-μm microsphere rather than the microsphere itself. Ten representative fields were counted.

To determine the inactivation rate of PRD-1 and M-1, approximately 50 mL of Borden groundwater was mixed with 10^4 pfu mL^{-1} of PRD-1 and M-1 and placed in a clean, sterile polypropylene centrifuge tube. The tube was placed in an 11°C water bath, and samples were taken and assayed daily. Levels of both PRD-1 and M-1 decreased about 25% over the 2-week period. We therefore assumed that over the course of the field experiment there was no significant loss of bacteriophage due to inactivation, consistent with past experience [*Yahya et al*., 1993].

Results

Experimental Breakthrough Curves

Figure 2 shows the injection history of PRD-1, M-1, microsphere, and electrical conductivity observed at the injection well during the attachment experiment. The assayed phage and microsphere injection concentrations fluctuated during the first injection period. For example, the PRD-1 concentration was 1.7×10^6 pfu mL^{-1} at the beginning and decreased to 3.6×10^5 near the end of the injection. Electrical conductivity and chloride concentration gradually decreased to their background values. Because the fluctuations of the different tracers in the injectate were not the same, causes of the fluctuations could not be attributed to a single factor. Insufficient mixing in the carboy and in the injection pipeline, fluctuations in the injection water pumping rate, and error in the enumeration of phages and microspheres were all possible contributors.

Breakthrough curves (Figure 3) obtained from the first experiment showed strong retention of colloids but also evidence of remobilization. Virus and microsphere concentrations at the two sampling wells were so low that complete PRD-1 and microsphere breakthrough curves were observed only at levels 6 and 8 of well ML4. That is, concentrations at other sampling points were near or below the detection limit during breakthrough. In this context a "complete" breakthrough curve means a concentration or electric conductivity versus time curve starting from the lower limit of concentration measurement, increasing gradually to a high concentration value, then decreasing gradually back to the lower limit of the measurement. The M-1 breakthrough curve was only complete at level 6 of ML4 and level 8 of ML5. Intermittent appearances of viruses and microspheres were evident at almost all of the eight points sampled in the two wells. Peak concentration values and times to peak, used to estimate the groundwater velocity in each layer, are given in Table 1. The highest PRD-1 concentrations were 440 pfu mL^{-1} at ML4 and 12 pfu mL^{-1} at ML5. Microspheres appeared at relatively higher concentrations than the two types of viruses. The highest microsphere concentrations were 2.8×10^5 mL^{-1} at ML4 and 4.7×10^4 mL^{-1} at ML5.

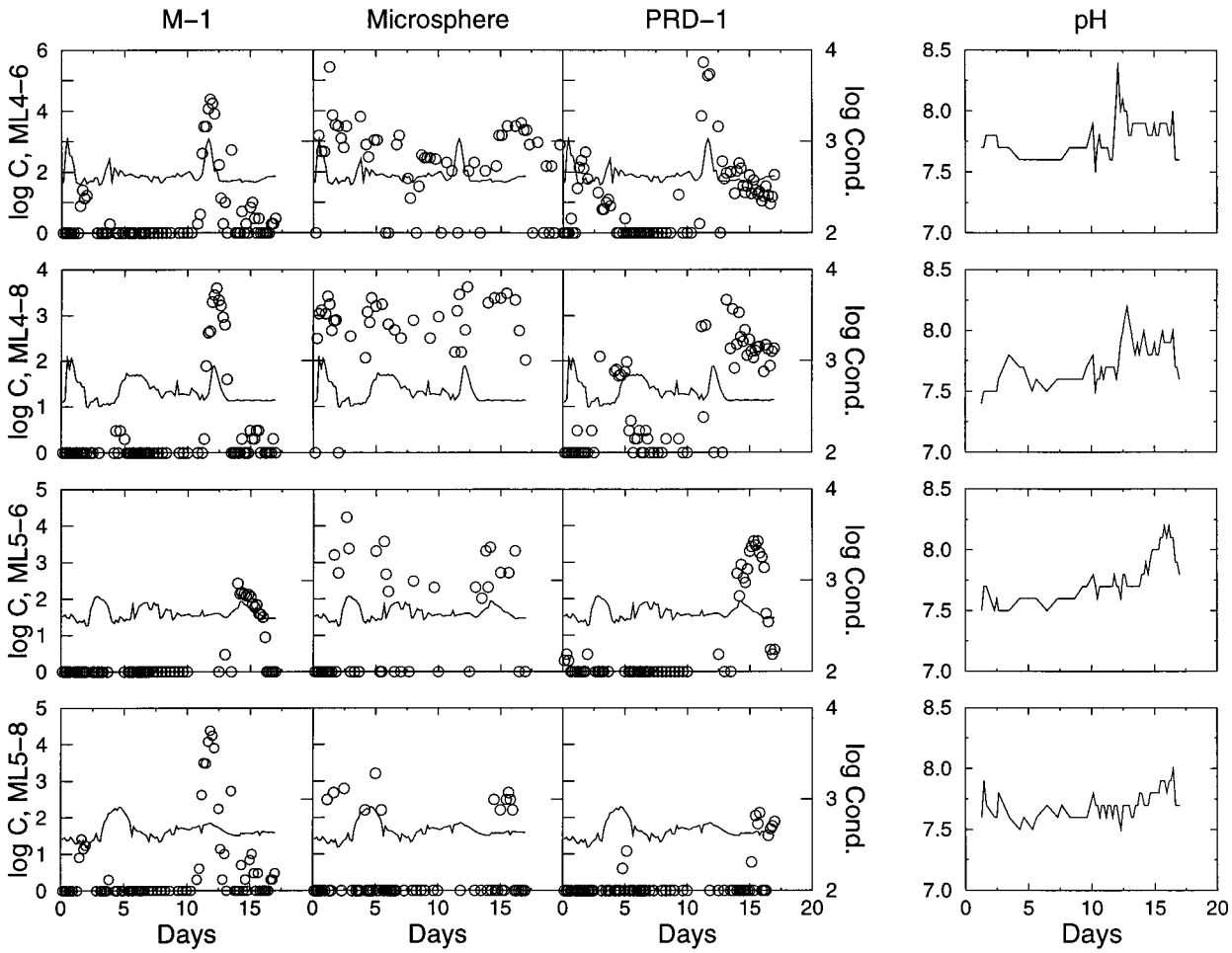

Figure 3. Injectate breakthroughs and *p*H at sampling levels 6 and 8 of wells ML4 and ML5 for both experiments. The first injection was at time = 0 and the second was at time = 11 days. Circles are colloid concentrations and lines are conductivity. Virus concentrations are in plaque-forming units per milliliter, microsphere is number per milliliter, and conductivity is microsiemons per centimeter. Samples below detection limit are plotted as C = 10°.

The times of appearance of the PRD-1 peaks were 3 to 6 times those for the conductivity peaks. For microspheres the lag was much less, about half a day (Table 1). The M-1 major peak also lagged the conductivity peak time. These delays in arrival of the breakthroughs indicate retardation of phage transport involving reversible retention and remobilization. The PRD-1 and M-1 peak concentration values at the sampling well 0.94 m downstream from the injection well were only

Table 1. Peak Information After the First Injection

			Conductivity†		PRD-1‡		M-1§		Microsphere‖	
Sampling Point	Depth, m	*p*H*	Time, days	Value, μS cm^{-1}	Time, days	Concentration, pfu mL^{-1}	Time, days	Concentration, pfu mL^{-1}	Time, days	Concentration, 10^3 mL^{-1}
ML4-3	2.3	7.5	0.8	1140	5.0	2	0.7	8	1.0	33
ML4-4	2.5	7.6	0.5	1050	5.0	8	1.2	5	1.2	9
ML4-5	2.7	7.7	0.5	1000	4.8	6	1.3	2	0.8	13
ML4-6	2.9	7.7	0.5	1070	1.8	440	1.7	26	1.0	275
ML4-8	3.3	7.6	0.5	1090	3.0	126	4.3	3	0.8	10
ML5-4	2.5	7.5	3.2	680	5.2	2	3.5	5	2.0	47
ML5-6	2.9	7.6	2.8	680	0.3	3	···	···	2.7	17
ML5-8	3.3	7.7	4.7	840	5.2	12	2.0	1	5.0	2

*Average before *p*H of the groundwater was modified.
†The highest electrical conductivity value at the injection well was 1160 μS cm^{-1}; background was 311 μS cm^{-1}.
‡The highest PRD-1 concentration at the injection well was 1.7×10^6 pfu mL^{-1}.
§The highest M-1 concentration at the injection well was 1.6×10^5 pfu mL^{-1}.
‖The highest microsphere concentration at the injection well was 1.1×10^8 mL^{-1}.

Table 2. Peak Information After the Second Injection

Sampling Point	Depth, m	pH*	Conductivity†		PRD-1		M-1		Microsphere	
			Time, days	Value, μS cm^{-1}	Time, days	Concentration, 10^3 pfu mL^{-1}	Time, days	Concentration, 10^3 pfu mL^{-1}	Time, days	Concentration, 10^3 mL^{-1}
ML4-3	2.3	8.0	12.5	650	12.0	0.3	11.5	1.3	12.0	0.5
ML4-4	2.5	8.5	11.7	1020	11.8	100	11.8	12.9	11.8	340
ML4-5	2.7	8.2	11.8	890	11.8	135	11.8	4.2	11.0	7.6
ML4-6	2.9	8.4	11.7	1060	12.2	1260	11.8	23.9	12.5	4.0
ML4-8	3.3	8.2	12.2	890	12.7	314	12.3	4.0	12.7	101
ML5-4	2.5	8.1	15.0	470	12.5	0.002	14.2	0.002	11.0	3.2
ML5-6	2.9	8.2	14.2	600	15.7	3.7	14.0	0.3	14.2	2.6
ML5-8	3.3	8.0	11.8	560	15.8	0.1	15.8	0.013	15.7	0.5

*The highest *p*H recorded at the injection well was 8.3.
†The highest conductivity at the injection well was 1654 μS cm^{-1}.

0.01% of the injection concentrations; at the second sampling well, 2.54 m downstream from the injection well, they were less than 0.001% of the injectate. The conservative tracer concentrations at the two sampling wells showed no similar decrease, ruling out dispersion as the main cause of the attenuation of colloid concentrations.

The electrical conductivity breakthrough curves (Figure 3) showed an initial breakthrough of the injectate, followed by a second unexplained peak; this second peak was apparently from another chloride source remaining from prior salt injection at the site.

Breakthrough curves from the second experiment (Figure 3) showed significant remobilization, followed by further transport and retention. There was no evident retardation of viruses and microspheres observed relative to the electrical conductivity. The times that peaks arrived at most points in ML4 and ML5 were nearly the same for the three colloids (Table 2). The highest PRD-1 concentrations caused by increasing the *p*H of groundwater were 1.3×10^6 pfu mL^{-1} at ML4 and 3.7×10^3 pfu mL^{-1} at ML5, 1000 times that observed during the attachment and transport test. For M-1 they were 2.4×10^4 pfu mL^{-1} at ML4 and 2.7×10^2 pfu mL^{-1} at ML5. The highest microsphere concentrations were 3.4×10^5 mL^{-1} at ML4 and 3.2×10^3 mL^{-1} at ML5. Fluctuations of *p*H and electrical conductivity were also observed during the injection (Figure 2), but the overall trend was consistent with the experimental adjustment, and therefore considered to be due to fluctuations in water supply rate. Note the two-step gradual rise in *p*H corresponding to the increase in *p*H first to 8.6 and then to 10.0 in the injectate. Figure 3 shows the observed *p*H changes at the two multilevel sampling wells. Values at most wells increased up to 0.5 *p*H unit. Note that *p*Hs in water withdrawn from the injection well were lower than those in the injectate owing to *p*H buffering by the soil and dilution.

Sampling at the extraction well showed nonzero phage concentrations in only one sample. Dilution at the extraction well undoubtedly caused concentrations to drop below the detection limit.

Modeling Phage and Microsphere Transport

Mas-Pla et al. [1992], *Yeh et al.* [1995a], and *McCarthy et al.* [1996] showed that correct estimation of physicochemical parameters for microorganism transport in the field demands an accurate description of groundwater velocity. This implies that three-dimensional modeling and detailed characterization of the experimental field site are necessary. During the 1980s a small portion of the Borden aquifer off the main experimental field site was extensively sampled for stochastic analysis of spatial variability of hydraulic conductivity [*Sudicky*, 1986]. This task aimed at deriving generic information about the heterogeneity at the Borden site. Using this generic information, many studies have tested macrodispersion concepts (i.e., assuming the aquifer is homogeneous) in the main portion of the aquifer. Results of the studies demonstrated that the generic information will be useful if and only if the tracer plume has traveled for a distance of hundreds to thousands of meters [e.g., *Sudicky*, 1986]. For small scale tracer tests such as our field experiment, one must rely on a site-specific description of the heterogeneity [e.g., *Yeh*, 1992; *Yeh et al.*, 1995b]. However, a detailed three-dimensional site characterization of our small-scale field site was not available. As a result, our analysis of the forced gradient test relies on a simplified one-dimensional flow and transport approach.

When molecular diffusion is much smaller than mechanical dispersion and rV = constant, where r and V are the distance from the injection well and velocity at r, *Bear* [1979] obtained a one-dimensional advection-dispersion equation for a plane radial transport problem. Since the injection rate in our field test was much smaller than that of the extraction rate, we can assume that the condition rV = constant was probably met for most of the r values and that the one-dimensional equation applies. When viral inactivation is not significant, one-dimensional transport can be described by a combined kinetic-equilibrium two-site model [*Cameron and Klute*, 1977; *Bales et al.*, 1991]:

$$\theta \frac{\partial C}{\partial t} + \rho_b \frac{\partial S_1}{\partial t} + \rho_b \frac{\partial S_2}{\partial t} = \theta \frac{\partial}{\partial x} D \frac{\partial C}{\partial x} - \theta \frac{\partial}{\partial x} uC \quad (1)$$

$$S_1 = K_{p1} C \quad (2)$$

$$\rho_b \frac{\partial S_2}{\partial t} = \theta k_1 C - \rho_b k_2 S_2 \quad (3)$$

$$D = \alpha_d u \quad (4)$$

where C is the concentration of viruses in groundwater, S_1 is concentration of those viruses attached on the fast (equilibrium) sites of soil surfaces, S_2 is concentration of those viruses attached on the slow (non-equilibrium) sites of soil surfaces, u is the interstitial groundwater velocity, D is the dispersion coefficient, K_{p1} is the equilibrium distribution coefficient for the equilibrium sites in cubic centimeters per gram, k_1 is the

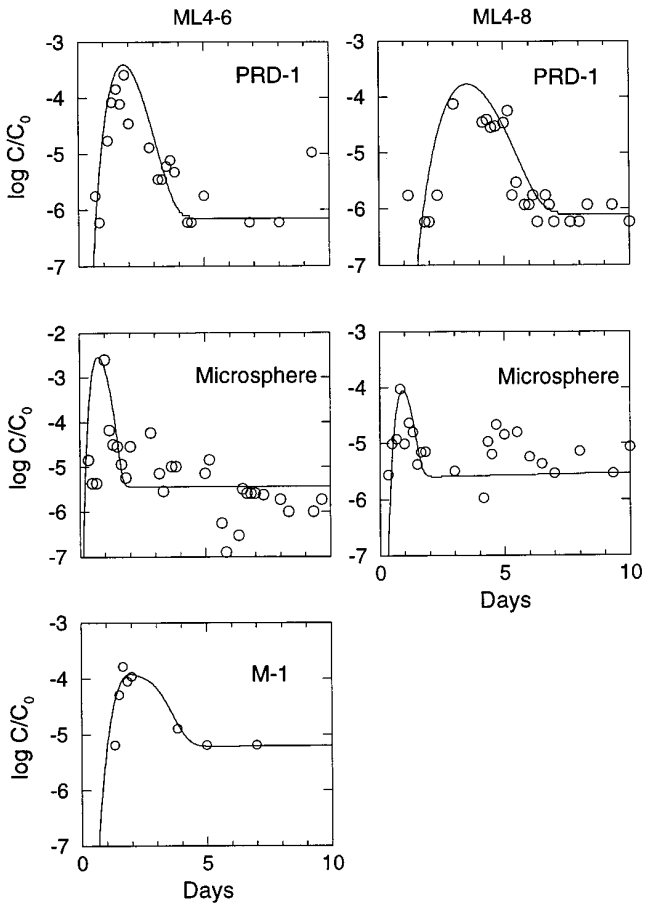

Figure 4. Colloid breakthrough curves for first injection fitted to the constant dispersivity model (attachment experiment). Circles are data, solid lines are simulations.

attachment rate constant for slow reaction sites, k_2 is the detachment rate constant for slow reaction sites, ρ_b is aquifer bulk density, θ is aquifer porosity, and α_d is the pore-scale dispersivity. The concentration of sites on the soil for viral or microsphere attachment is assumed to be large relative to the concentration of the viruses and microspheres and therefore does not appear in (2) and (3).

Equations (1)–(4) were used to describe the attachment experiment. The same model but with different parameters was used to describe the detachment experiment, that is, after the chemical disturbance. This was based on three assumptions: (1) strong colloid detachment started at a point only after the pulse of high-pH water had arrived at that point, (2) strong colloid detachment ceased after the pulse had passed that point, and (3) the high-pH water had residual effects on the surfaces of soil particles and colloids such that reattachment of colloids at that point proceeded at a rate different from that previously. These assumptions required all rate constants in the previous governing equations (2) and (3) to be treated as functions of time:

$$K_p = \begin{cases} K_{p11} & t < t_x \text{ or } t > t_x + t_0 \\ K_{p12} & t_x \le t \le t_x + t_0 \end{cases} \quad (5)$$

$$k_1 = \begin{cases} k_{11} & t < t_x \text{ or } t > t_x + t_0 \\ k_{12} & t_x \le t \le t_x + t_0 \end{cases} \quad (6)$$

$$k_2 = \begin{cases} k_{21} & t < t_x \text{ or } t > t_x + t_0 \\ k_{22} & t_x \le t \le t_x + t_0 \end{cases} \quad (7)$$

$$t_x = \int_0^x \frac{dx}{u(x)} \quad (8)$$

The second 1 in the above subscripts stands for the rate and equilibrium constants valid before the chemical disturbance arrived at (time t_x) or after it passes (time $t_x + t_0$) by a given point; the 2 represents the variable valid during the period of chemical disturbance.

Curve fitting was used to estimate and evaluate the chemical parameters of the phage and microsphere transport at the field site. Numerical solutions to the governing equations were first derived using a finite difference method. The time and space intervals were chosen so that the Courant number was less than 1 and the local Peclet number was less than 2. The time factor for the implicit finite difference equation was 0.6.

The velocity formula

$$v(x) = -\frac{K}{\theta}\frac{\partial s}{\partial x} = \frac{1}{2\theta\pi h_0}\left(\sum_1^n \frac{Q_j(x - x_j)}{r_j^2} - \sum_1^m \frac{Q_i(x - x_i)}{r_i^2}\right) \quad (9)$$

was used in curve fitting. In these equations h_0 is the aquifer thickness, x is the coordinate along a distance r from the pumping well, r is the distance between a well and a point where velocity is to be calculated, and θ is the aquifer porosity. In deriving (9) the aquifer has been treated as homogeneous and isotropic so that θ and K do not vary with x and aquifer depth. Equation (9) is exactly the same as that when h is defined as potential [*Javandel et al.*, 1984]. Equation (9) was developed from fitting a Strack potential model [*Strack*, 1985; *de Marsily*, 1986] to the head data from the observation wells and piezometers [*Li*, 1993]. We also evaluated use of a delayed response of water table model [*Neuman*, 1975] and a Theis model [e.g., *Freeze and Cherry*, 1979], but neither gave a good fit to drawdown data [*Li*, 1993]. Flow rates for an individual level were varied to obtain the best fit. Dispersivity estimates (0.1–0.6 m at ML4) were derived from fitting electrical conductivity breakthrough curves [*Li*, 1993].

Fitting was conducted only on the complete breakthrough curves, with results for the first experiment shown on Figure 4. Fitted chemical parameters for both attachment and detachment experiments are given in Table 3. The simulated colloid concentrations in soil at day 10 of the attachment experiment were used as input for the simulation of detachment experiment. The fitting results of the detachment breakthrough curves are shown in Figure 5.

We also predicted colloid breakthrough curves at sampling well ML5 using the parameters from ML4. Such a prediction depended on successful simulation of both the attachment and detachment experiments at ML4. The prediction at ML5 for the detachment experiment was in agreement with the observed timing of breakthrough (Figure 6). Both predicted and observed colloid concentrations were not zero. The predicted peak times were near the observed ones. The differences between predicted and observed peak concentrations were within a factor of 10. The model prediction for the attachment experiment is not shown, since observed breakthrough curves were incomplete.

Table 3. Fitted Equilibrium and Rate Constants

Colloid	ML Location	Experiment	k_1 day^{-1}	k_{12} day^{-1}	k_2 day^{-1}	k_{22} day^{-1}	k_3	k_{32}
PRD-1	4-6	att.	10.7	···	0.0003	···	2.05	···
PRD-1	4-6	det.	10.7	6.0	0.0003	15.0	0.25	0.25
PRD-1	4-8	att.	6.1	···	0.0004	···	2.12	···
PRD-1	4-8	det.	10.7	3.0	0.0050	17.0	1.05	1.05
M-1	4-6	att.	10.0	···	0.0050	···	2.35	···
M-1	4-6	det.	10.7	6.0	0.0005	8.0	0.25	0.25
Microsphere	4-6	att.	7.0	···	0.0005	···	0.05	···
Microsphere	4-6	det.	7.0	3.0	0.0005	0.006	1.55	1.55
Microsphere	4-8	att.	11.2	···	0.0070	···	0.35	···
Microsphere	4-8	det.	10.5	2.07	0.0080	1.0	1.25	1.25

Here att., attachment; det., detachment.

Discussion

At both wells the microspheres were retarded less than were the two phages. The largest microsphere concentration values observed at ML4 were delayed 0.7 days relative to the electric conductivity, versus a delay of up to several days for PRD-1 and M-1. At ML5, the largest microsphere concentration occurred before electric conductivity peaks at levels ML5-4 and ML5-6, and only 0.33 days behind at level ML5-8. *Harvey et al.* [1989] observed a similar range of behavior in their natural-gradient study of microsphere and bacteria transport. In one case the peak bacteria concentration was observed before the peak for conservative solute, whereas the peak microsphere concentration lagged the solute peak. Concentrations of both colloids were attenuated. Colloid attenuation over the first meter of transport was a factor of 10^4–10^7 for PRD-1 and microspheres, respectively, a level that should be indicative of transport of these colloids over longer times. Attenuation over the next 2 m was approximately a factor of 10. These results are consistent with our previous natural-gradient transport experiment at Cape Cod in which most of the attenuation occurred between the injection and first observation wells [*Bales et al.*, 1995].

After the injection of the high-pH water the dimensionless PRD-1, M-1, and microsphere peak concentrations were 0.74, 0.15, and 0.003 at sampling well ML4 and 0.002, 0.002, and 3×10^{-5} at ML5, respectively. These observations showed that (1) attached phages detached at high rates and reentered the moving groundwater, (2) PRD-1 detached more readily than did M-1 or the microspheres, and (3) phages that reentered the moving groundwater reattached to porous media as they were transported downstream. Because the colloids observed at ML4 and ML5 in the second experiment were from various points between the injection well and sampling points, we could not accurately assess retardation in the second experiment.

The combined kinetic-equilibrium two-site model was found to be adequate to simulate colloid attachment and transport processes (Figure 4). The k_1 mainly affects the peak value of a breakthrough curve. The k_2 mainly influences the level of the tail of the breakthrough. The ratio k_1/k_2 controls the slope of both the rising concentration and dropping limbs of a breakthrough curve. The k_3 affects the peak position for a given flow rate and the width of the breakthrough curves as well. The attachment rate constants of PRD-1, M-1, and microspheres

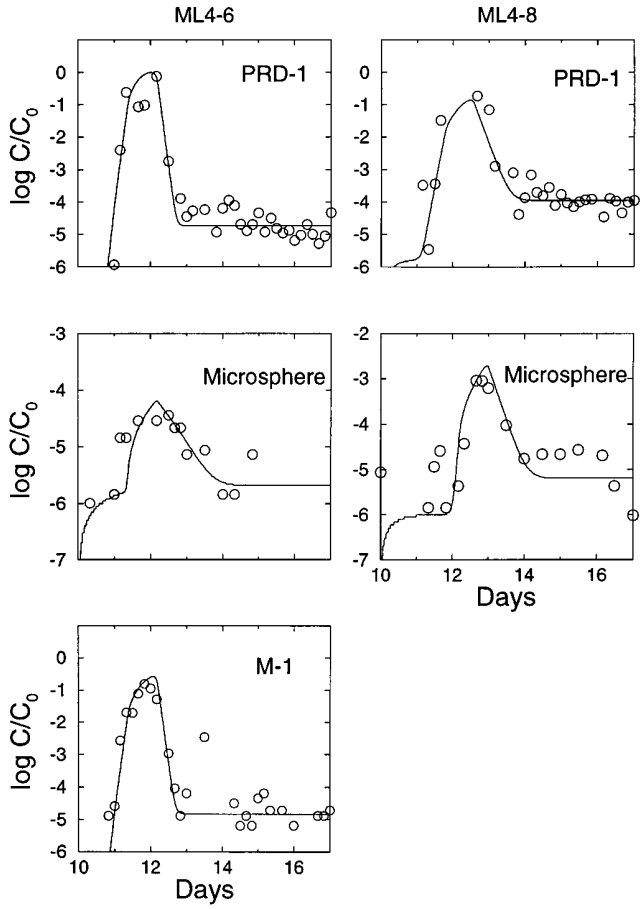

Figure 5. Colloid breakthrough curves for second injection fitted to the constant dispersivity model (detachment experiment). Circles are data, solid lines are simulations.

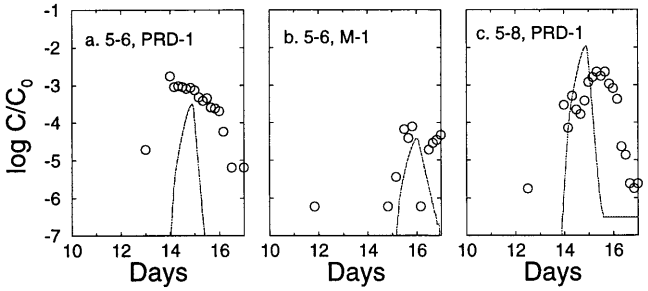

Figure 6. Comparison between observed and predicted colloid breakthrough curves for detachment experiment at ML5.

were 10,000–100,000 times the corresponding detachment rate constants, showing that attachment dominated (Table 3).

We previously reported a k_1 value for PRD-1 removal in laboratory column studies with soil from the site of about 100 day^{-1} [*Kinoshita et al*., 1993], 10 times the value estimated in the current work. Velocity and *p*H in lab studies were the same as in the current work, so this difference shows directly that phage removal in the field was only 10% as efficient as with repacked soil columns. Some difference may be attributed to spatial heterogeneity in soil chemical properties. That is, the soil used in the soil columns was from near the site of the experiment, but may not be representative of the area of the experiment. Some if not most of the difference can also be attributed to the use of repacked soil versus physically heterogeneous field media. Mean arrival times for the conservative tracer peak were relatively consistent in our experiment (ML4, Table 1) but varied by ±35% in a previous experiment at the site [*Mackay et al*., 1994].

Similarly, *Mas-Pla et al*. [1992] reported that the estimated porosity value from one-dimensional analysis of a forced-gradient tracer experiment is physically unreasonable. They attributed the discrepancy to the fact that the one-dimensional flow and transport does not capture three-dimensional flow and transport phenomena in the field. As a result, the parameter values estimated from the one-dimensional analysis likely include effects neglected by the simplified analysis.

Application of our transport model to the second experiment, where the colloid detachment rate was higher than in the first experiment, required considering the length of time the chemical disturbance had an effect at any given point. Fast colloid detachment occurred when the chemical disturbance, a short duration of high-*p*H water, passed a point. The strength of a disturbance and the equilibrium and rate constants depended on the *p*H value. Groundwater *p*H at a given sampling point varied up and down during the detachment experiment; thus *p*H values at ML5 were about the same as those at ML4 (Figure 3). The equilibrium and first-order rate constants were assumed to vary in response to changes in *p*H, as shown by (5)–(7).

Figure 5 shows that the combined equilibrium and kinetic model can also simulate the general pattern of the detachment and transport processes. In addition to the roles discussed above, k_{11}, the first-order attachment rate constant for the times before and after the action of chemical disturbance at a given spatial point, affects the concentration level and timing of the beginning part of a breakthrough curve; k_{22}, the first-order detachment rate constant during the action of the chemical disturbance, mainly controls the peak values. The PRD-1 detachment rate constant during the chemical disturbance was 10^6 times that in the attachment experiment and of the same order as but higher than the attachment rate constant. The rate constants for M-1 phage indicated the same relationship. For microspheres, the detachment rate constant was 10–1000 times that in the attachment experiment but did not exceed the attachment rate constant. Microsphere detachment was weaker as compared to the two phages. The microsphere equilibrium adsorption constant (k_3) for the detachment experiment was 10–100 times that in the attachment experiment; the phage equilibrium adsorption constant decreased by about 90%, showing again that microspheres behaved differently from the phage. The lower attachment rate constants k_{11} (Table 3) during the detachment experiment shows the residual effect of the pulse of high-*p*H water, that is, changing the soil and colloid surface chemistry.

During the attachment and transport experiment the attachment of colloids was fast and detachment was very slow compared to advection. Using the conductivity peak information in Table 1, the average velocity (over the distance from the injection well to the ML4 sampling well) was 1.9 m d^{-1}. The timescale of colloid attachment relative to advection (u/k_1L) was 0.095 for PRD-1, 0.074 for M-1, and 0.088 for microspheres, where L is the distance between wells. The relative time scale for detachment (u/k_2L) was 2200 for PRD-1, 1500 for M-1, and 800 for microspheres.

During the detachment experiment the detachment of colloids was fast and attachment kept about the same rate as those in the attachment experiment. Using the conductivity peak information in Table 2, the average velocity was 0.4 m d^{-1}. The timescale ($u/k_{22}L$) was 0.01 for PRD-1, 0.02 for M-1, and 13.2 for microspheres. These detachment timescales were much smaller than those in the attachment experiment, varying from 0.0004% for PRD-1, 0.013% for M-1, to 1.7% for microspheres.

Conclusions

As shown by our modeling of the field experiment of biocolloid transport, a one-dimensional transport model with first-order kinetic plus an equilibrium mass-transfer term was adequate to describe the biocolloid mass-transfer processes between the soil and water phases of the aquifer. The transport of viruses and bacteria from sources such as septic tanks or sewage lines can therefore be simulated with the advection-dispersion equation coupled with the simple mass transfer equations. However, our estimated coefficients for virus attachment to soil particles, and thus log removal per length, were only one tenth those found in lab studies. Since our one-dimensional model assumed homogeneity and neglects the effect of the partially penetrating well (5-m screen interval), our model greatly simplified the tortuous three-dimensional flow regime in the aquifer. Thus some discrepancy between the parameter values of laboratory experiments and those of field tests is expected [*Yeh*, 1992; *McCarthy et al*., 1996]. This discrepancy highlights the large uncertainty that will ensue using a one-dimensional model with laboratory-determined parameters. To properly interpret the chemical tracer data under field conditions, three-dimensional site characterization of aquifer heterogeneity and modeling [*Yeh et al*., 1995a, b] may be necessary.

In spite of possible errors due to the one-dimensional analysis, we clearly showed that colloid attachment to the soil matrix followed by slow (relative to advective timescale) release of retained colloids was more important than was reversible "equilibrium" adsorption, because adsorption characterized by fast uptake and slow release controlled the final colloid concentration levels in both soil and groundwater. Equilibrium adsorption on the timescale of the experiment contributed only to a slight retardation of colloids and had a minor effect on concentration.

The pulse of high-*p*H water was introduced at the injection well as a chemical disturbance traveled downstream with the groundwater. The action of this chemical disturbance (causing detachment in our case) at a given point downstream started when it arrived at that point and ended when it passed by. When the major action was to cause detachment of previously

attached colloids, as in our case, further downstream transport of colloids was facilitated. The rate of release of retained colloids caused by a chemical disturbance was 100 to 10^6 times that of the unperturbed release. The detachment and further downstream transport of colloids can be simulated with the same type of model used for the attachment and transport process, provided the *p*H dependence of the rate constants is included.

Finally, prediction of bulk behavior of virus transport is possible with appropriate estimates of physicochemical parameters, primarily attachment and detachment rate coefficients; simply knowing a "retardation factor" is not sufficient. Exact prediction of transport, such as the number of viruses occurring at a certain point downstream from a source, may not be feasible considering the heterogeneity of aquifer in its physicochemical qualities. But order-of-magnitude estimates may be sufficient for engineering solutions to biocolloid transport problems. Results of recent controlled field experiments and detailed three-dimensional modeling efforts by *Yeh et al.* [1995a, b] support this conclusion.

Acknowledgments. The project described was supported in part by funding from the U.S. Environmental Protection Agency's (EPA) Robert S. Kerr Environmental Research Laboratory in Ada, Oklahoma, through grant CR-818113, with additional support from grant P42ES04940 from the National Institute of Environmental Health Sciences, NIH. This paper does not necessarily reflect the views of the NIH or EPA. We also acknowledge the generous support of D. Mackay and J. Cherry for giving us use of the site and G. Bianchi-Mosquera for cooperation in carrying out the experiment. R. Brice assisted in manuscript preparation.

References

Adams, M. H., *Bacteriophages*, Interscience, New York, 1959.

Bales, R. C., S. R. Hinkle, T. W. Kroeger, K. Stocking, and C. P. Gerba, Bacteriophage adsorption during transport through porous media: chemical perturbations and reversibility, *Environ. Sci. Technol.*, *25*, 2088–2095, 1991.

Bales, R. C., S. Li, K. Maguire, M. Yahya, and C. P. Gerba, MS-2 phage and poliovirus transport through porous media: sorbent hydrophobicity and chemical perturbations, *Water Resour. Res.*, *29*, 957–963, 1993.

Bales, R. C., S. Li, K. M. Maguire, M. T. Yahya, C. P. Gerba, and R. W. Harvey, Virus and bacteria transport in a sandy aquifer, Cape Cod, MA, *Ground Water*, *33*(4), 653–661, 1995.

Bamford, D. H., L. Rouhiainen, K. Takkinen, and H. Söderlund, Comparison of the lipid-containing bacteriophages PRD1, PR3, PR4, PR5 and L17, *J. Gen. Virology*, *57*, 365–373, 1981.

Bamford, D. H., J. Caldentey, and J. K. H. Bamford, Bacteriophage PRD1: A broad host range DSDNA tectivirus with an internal membrane, *Adv. Virus Res.*, *45*, 281–319, 1995.

Bear, J., *Hydraulics of Groundwater*, 721 p., McGraw-Hill, New York, 1979.

Cameron, D., and A. Klute, Convective-dispersive solute transport with combined equilibrium and kinetic adsorption model, *Water Resour. Res.*, *13*, 183–188, 1977.

Corapcioglu, M. Y., and A. Haridas, Transport and fate of microorganisms in porous media: a theoretical investigation, *J. Hydrol.*, *72*, 149–169, 1984.

Corapcioglu, M. Y., and A. Haridas, Microbial transport in soils and groundwater: A numerical model, *Adv. Water Resour.*, *8*, 188–200, 1985.

de Marsily, G., *Quantitative Hydrogeology*, Academic, San Diego, Calif., 1986.

Frankel-Conrat, H., P. C. Kimball, and J. A. Levy, *Virology*, Prentice Hall, Englewood Cliffs, N. J., 1988.

Freeze, R., and J. Cherry, *Groundwater*, Prentice Hall, Englewood Cliffs, N. J., 1979.

Funderburg, S. W., B. E. Moore, B. P. Sagik, and C. A. Sorber, Viral transport through soil columns under conditions of saturated flow, *Water Res.*, *15*, 703–711, 1981.

Gerba, C. P., Applied and theoretical aspects of virus adsorption to surfaces, *Adv. Appl. Microbiol.*, *30*, 133–168, 1984.

Gerba, C. P., M. V. Yates, and S. R. Yates, Quantitation of factors controlling viral and bacterial transport in the subsurface, in *Modeling the Environmental Fate of Microorganisms*, edited by C. J. Hurst, pp. 77–88, Am. Soc. for Microbiol., Washington, D. C., 1991.

Grosser, P. W., A one-dimensional mathematical model of virus transport, in *Proceedings of the Second International Conference on Groundwater Quality Research*, pp. 105–107, Univ. Ctr. for Water Res., Okla. State Univ., Stillwater, 1985.

Harvey, R., Parameters involved in modeling movement of bacteria in groundwater, in *Modeling the Environmental Fate of Microorganisms*, edited by C. J. Hurst, Am. Soc. for Microbiol., Washington, D. C., 1991.

Harvey, R. W., and S. P. Garabedian, Use of colloid filtration theory in modeling movement of bacteria through a contaminated sandy aquifer, *Environ. Sci. Technol.*, *25*, 178–185, 1991.

Harvey, R., L. H. George, R. L. Smith, and D. R. LeBlanc, Transport of microspheres and indigenous bacteria through a sandy aquifer: Results of natural and forced-gradient tracer experiments, *Environ. Sci. Technol.*, *23*, 51–56, 1989.

Hobbie, J. E., R. J. Daley, and S. Jasper, Use of nuclepore filters for counting bacteria by fluorescence microscopy, *Appl. Environ. Microbiol.*, *33*, 1225–1228, 1977.

Javandel, I., C. Doughty, and C. F. Tsang (Eds.), *Groundwater Transport: Handbook of Mathematical Models*, *Amer. Geophys. Union*, *Water Res. Monogr.*, vol. 10, AGU, Washington, D. C., 1984.

Kinoshita, T., R. C. Bales, M. T. Yahya, and C. P. Gerba, Effect of *p*H on bacteriophage transport through sandy soils, *J. Contam. Hydrol.*, *15*, 55–70, 1993.

Li, S., Modeling biocolloid transport in saturated porous media, Ph.D. thesis, Univ. of Ariz., Tucson, 1993.

MacFarlane, D. S., J. A. Cherry, R. W. Gillham, and E. A. Sudicky, Migration of contaminants in groundwater at a land fill: A case study, 1, Groundwater flow and plume delineation, *J. Hydrol.*, *63*, 1–29, 1983.

Mackay, D. M., G. Bianchi-Mosquera, A. A. Kopania, H. Kianjah, and K. W. Thorbjarnarson, A forced-gradient experiment on solute transport in the Borden aquifer, 1, Experimental methods and moment analyses of results, *Water Resour. Res.*, *30*(2), 369–383, 1994.

Mackay, D. M., D. L. Freyberg, P. V. Roberts, and J. A. Cherry, A natural gradient experiment on solute transport in a sand aquifer, 1, Approach and overview of plume movement, *Water Resour. Res.*, *22*, 2017–2029, 1986.

Mas-Pla, J., T.-C. J. Yeh, J. F. McCarthy, and T. M. Williams, Numerical simulation of a two-well tracer experiment, *Ground Water*, *30*(6), 958–964, 1992.

Matthes, G., A. Pekdeger, and J. Schroeter, Persistence and transport of bacteria and viruses in groundwater—a conceptual evaluation, *J. Comtam. Hydrol.*, *2*, 171–188, 1988.

McCarthy, J. F., B. Gu, L. Liang, J. Mas-Pla, T. M. Williams, and T.-C. J. Yeh, Field tracer tests on the mobility of natural organic matter in a sandy aquifer, *Water Resour. Res.*, *32*(5), 1223–1238, 1996.

McCaulou, D. R., R. C. Bales, and R. G. Arnold, Effect of temperature-controlled motility on transport of bacteria and microspheres through saturated sediment, *Water Resour. Res.*, *31*(2), 271–280, 1995.

Neuman, S. P., Analysis of pumping test data from anisotropic unconfined aquifers considering delayed gravity response, *Water Resour. Res.*, *11*, 329–342, 1975.

Olsen, R. H., J. Siak, and R. Gray, Characteristics of PRD1, a plasmid-dependent broad host range DNA bacteriophage, *J. Virology*, *14*, 689–699, 1974.

Strack, O. D. L., *Groundwater Mechanics*, Prentice Hall, Englewood Cliffs, N. J., 1985.

Sudicky, E. A., A natural gradient experiment on solute transport in a sand aquifer: Spatial variability of hydraulic conductivity and its role in the dispersion process, *Water Resour. Res.*, *22*(13), 2069–2082, 1986.

Vilker, V. L., An adsorption model for prediction of virus breakthrough from fixed beds, in *State of Knowledge in Land Treatment of Wastewater*, vol. 2, edited by H. L. McKim, pp. 381–388, U.S. Army Cold Reg. Res. and Eng. Lab., Hanover, N. H., 1978.

Vilker, V. L., and W. D. Burge, Adsorption mass transfer model for virus transport in soils, *Water Res*., *14*, 783–790, 1980.

Yahya, M., L. Galsiomes, C. P. Gerba, and R. C. Bales, Survival of bacteriophages MS-2 and PRD-1 in ground water, *Water Sci. Technol*., *27*, (3–4), 409–412, 1993.

Yates, M. V., S. R. Yates, J. Wagner, and C. P. Gerba, Modeling virus survival and transport in the subsurface, *J. Contam. Hydrol*., *1*, 329–345, 1987.

Yeh, T.-C. J., Stochastic modeling of groundwater flow and solute transport in aquifers, *J. Hydrol. Process*., *6*, 369–395, 1992.

Yeh, T.-C. J., J. Mas-Pla, J. F. McCarthy, and T. M. Williams, Modeling of natural organic matter transport processes in groundwater, *Environ. Health Perspect*., *108* (suppl. I), 41–46, 1995a.

Yeh, T.-C. J., J. Mas-Pla, T. M. Williams, and J. F. McCarthy, Observation and three-dimensional simulation of chloride plume in a sandy aquifer under forced-gradient conditions, *Water Resour. Res*., *31*(9), 2141–2157, 1995b.

R. C. Bales and T.-C. J. Yeh, Department of Hydrology and Water Resources, University of Arizona, Box 210011, Tucson, AZ 85721. (e-mail: roger@hwr.arizona.edu)

C. P. Gerba, Department of Soil, Water, and Environmental Science, University of Arizona, Tucson, AZ 85721.

M. E. Lenczewski, Amway Corp., 7575 Fulton St. E 50-2D, Ada, MI 49355-0001.

S. Li, Arizona Department of Environmental Quality, 3033 North Central Avenue, Phoenix, AZ 85012.

(Received April 22, 1996; revised December 31, 1996;
accepted December 31, 1996.)